arXiv:cond-mat/0303372v1 [cond-mat.supr-con] 19 Mar 2003

Point contact spectroscopy of the electron-doped cuprate superconductor $Pr_{2-x}Ce_xCuO_4$: The dependence of conductance-voltage spectra on cerium doping, barrier strength and magnetic field

M. M. Qazilbash, Amlan Biswas, Y. Dagan, R. A. Ott and R. L. Greene
Center for Superconductivity Research, Department of Physics, University of Maryland, College Park, MD-20742
(March 22, 2022)

Abstract

We present conductance-voltage ($G-V$) data for point contact junctions between a normal metal and the electron doped cuprate superconductor $Pr_{2-x}Ce_xCuO_4$ (PCCO). We observe a zero bias conductance peak (ZBCP) for the under-doped composition of this cuprate ($x = 0.13$) which is consistent with d-wave pairing symmetry. For optimally-doped ($x = 0.15$) and over-doped ($x = 0.17$) PCCO, we find that the $G-V$ characteristics indicate the presence of an order parameter without nodes. We investigate this further by obtaining point contact spectroscopy data for different barrier strengths and as a function of magnetic field.

PACS No.s 74.80.Fp, 74.25.Jb, 74.50.+r, 74.76.Bz

Typeset using REVTEX

I. INTRODUCTION

Point contacts between a normal metal and a superconductor have been extensively employed to probe the quasiparticle states of superconductors near the Fermi energy. Point contact spectroscopy (PCS) experiments have also been done to investigate the pairing symmetry of superconductors and the presence or absence of nodes in the superconducting order parameter [1]. In particular, in the hole doped copper oxide high T_c superconductors (HTSC), PCS and junction tunneling experiments have shown that the pairing symmetry is predominantly d-wave [2], strongly supporting the results of many other types of experiments [3]. Some of the tunneling experiments have even suggested a doping-dependent order parameter and the existence of a Quantum Critical Point (QCP) near optimum doping [4]. In the electron doped (n-doped) HTSC, the prior PCS and tunneling data has been more controversial and there is no consensus at present on the implications of the data. The reason is the absence of a zero bias conductance peak (ZBCP) in the tunneling spectra [5–7] which argues against the presence of d-wave pairing symmetry while other types of experiments [8–10] support a d-wave pairing symmetry. In this paper, we present more detailed PCS experiments on the n-doped HTSC $Pr_{2-x}Ce_xCuO_4$ (PCCO) in an attempt to better understand the pairing symmetry in the n-doped HTSC at all doping levels.

The theory of quasiparticle tunneling in a point contact junction between a normal metal and a conventional BCS-type superconductor has been developed by Blonder, Tinkham and Klapwijk (BTK) [11]. In the BTK model, the superconductor is assumed to have an isotropic gap in momentum space. The barrier between the normal metal and superconductor is modelled by a delta function. The strength of the delta function is characterized by a dimensionless parameter Z. The $Z = 0$ limit signifies a completely transparent junction while $Z >> 1$ is the tunneling limit. This model has been very successful in explaining the features of the $G - V$ spectra for tunneling in conventional s-wave superconductors [12]. Fig. 1a shows calculated $G - V$ characteristics for different barrier strengths.

The BTK model has been modified by Tanaka and Kashiwaya [13] for tunneling in superconductors with d-wave symmetry of the order parameter. The gap in a superconductor with d-wave symmetry is of the form $\Delta_{\mathbf{k}}=\Delta_0 \mathrm{Cos}(2\theta_{\mathbf{k}})$ where $\theta_{\mathbf{k}}$ is the angle of a wave vector on the Fermi surface relative to [100]. The order parameter is anisotropic and changes sign in momentum space. Constructive interference between the electron-like and hole-like quasiparticles, which experience different signs of the order parameter, results in formation of surface bound states at the Fermi energy [14]. These surface bound states are also referred to in the literature as Andreev bound states (ABS) and lead to enhancement of tunneling conductance at zero bias. The ZBCP is expected for tunneling into the ab-plane for all surfaces except (100) and (010). The ZBCP reaches maximum height for tunneling into (110) family of planes and Fig. 1b shows the tunneling spectra for such case. The $G-V$ tunneling spectra in d-wave superconductors are direction-dependent assuming a specular interface between the normal metal and superconductor. However, in practice the surface of the superconductor is rough on the atomic scale and this results in contribution to the tunneling current from facets of various orientations. When the effect of surface roughness is taken into account [15], the $G - V$ spectra for tunneling into (100) and (010) planes also exhibit a ZBCP. ZBCPs have been observed in hole-doped HTSC, most notably and consistently in $YBa_2Cu_3O_{7-\delta}$ (YBCO) for tunneling both into (100) and (110) orientations

[4,16,17].

The order parameter symmetry may be more complicated than simply s-wave or d-wave, especially at the surface. This is of relevance because PCS essentially probes surface electronic states. The theory for tunneling into superconductors with more complex pairing symmetries, for example, anisotropic s-wave, extended s-wave and $d + is$ has also been developed [18].

While most of the cuprate superconductors have holes as their charge carriers, the family of cuprate superconductors $R_{2-x}Ce_xCuO_4$ (R = La, Nd, Pr, Sm, Eu) is unique in the sense that its carriers are predominantly electrons. Several early tunneling spectroscopy and PCS experiments were performed on optimally-doped $Nd_{1.85}Ce_{0.15}CuO_4$ (NCCO) [5–7] to investigate the density of states and pairing symmetry of this compound. All these experiments revealed a gap-like feature in the $G - V$ spectra of NCCO with no hint of a ZBCP due to ABS. This led to the conclusion that the pairing symmetry for NCCO was not d-wave but either conventional or anisotropic s-wave, in stark contrast to the hole-doped HTSCs. However, two recent PCS and Scanning Tunneling Spectroscopy (STS) experiments have observed ZBCP in optimally-doped NCCO [20,21]. Recently, we presented PCS data on under-doped PCCO which provided convincing evidence for a ZBCP due to ABS [22]. In that work, evidence for a doping-dependent pairing symmetry was also presented.

Meanwhile, penetration depth experiments on NCCO also supported the s-wave scenario [23–25]. However, it was later realized that the magnetic moment of the Nd^{3+} ions would influence these measurements and might point to a misleading conclusion. Subsequent experiments on the related optimally-doped compound, PCCO [9,10], which is not plagued by the magnetic moment problem, provide evidence for d-wave symmetry. However, other penetration depth experiments on optimally-doped PCCO and NCCO [26,27] are more consistent with s-wave pairing symmetry. The work of Skinta *et al.* [27] also presents evidence for a doping dependence of the pairing symmetry.

Strong evidence of d-wave symmetry for optimally-doped NCCO and PCCO was provided by the phase sensitive tri-crystal grain boundary junction (GBJ) experiment [8], angle-resolved photoemission (ARPES) measurements [28,29] and Raman spectroscopy [30]. However, these experiments, like tunneling and penetration depth measurements, are to some extent sensitive to the surface of the sample and there is the issue that the surface may be different from the bulk. Moreover, the doping near the grain boundaries may be different from that in the bulk and could influence the results of the tri-crystal GBJ and the GBJ tunneling experiments. Measurements of bulk properties were expected to finally resolve the question of the pairing symmetry but the results have yet to converge. A very small residual linear term in thermal conductivity measurements of PCCO crystals is evidence for absence of nodes in the gap and does not lend support to a pure d-wave pairing symmetry [31]. Several explanations have been put forward for the absence of the residual linear term including the presence of a complex order parameter and localization of d-wave quasiparticles. The other bulk measurement, specific heat, argues in favor of dirty d-wave pairing symmetry [32]. The term 'dirty d-wave' refers to a d-wave pairing symmetry in a superconductor which contains impurities leading to physical properties that deviate from those of a clean d-wave superconductor.

To summarize, despite strong evidence for a d-wave symmetry, there is no consensus on the nature of the pairing symmetry in optimally doped PCCO and NCCO. The most

recent PCS and penetration depth data favors a doping-dependent pairing symmetry for these materials: d-wave for under-doped and s-wave for over-doped. In this paper we carry out an extensive investigation with PCS on PCCO thin films below their superconducting transition temperatures (T_c). We study the $G-V$ characteristics as a function of cerium doping, magnetic field and barrier strength (Z).

II. EXPERIMENTAL METHOD

PCCO thin films were used for PCS because better control and homogeneity of cerium is achieved in thin films compared to ceramic samples and single crystals. We have grown c-axis oriented PCCO thin films on Strontium Titanate (STO) and Lanthanum Aluminate (LAO) substrates using pulsed laser deposition. Details of film growth have been published elsewhere [33,34]. Superconducting thin films of PCCO with cerium concentrations of 0.13 (under-doped), 0.15 (optimally-doped) and 0.17 (over-doped) were grown. The films have a thickness of $2500-3000\mathring{A}$. The films were characterized by resistivity, AC susceptibility and X-ray diffraction measurements. The T_c for the under-doped, optimally-doped and over-doped films as determined from AC susceptibility and resistivity measurements are in the range $12\pm1K$, $21\pm0.5K$ and $14\pm1K$ respectively.

The 'spear on anvil' technique is widely used for making the point contact junction. A sharp metal tip is carefully brought into contact with the superconductor and the barrier strength is controlled by varying the pressure of the contact with a screw mechanism or a transducer (see, for example, the reviews in Ref. [35,36]). In some cases, the sharp tip of a superconducting material has been employed with the normal metal as the counter electrode [12]. However, this method is difficult to implement in our experiment for the following reasons. Only c-axis superconducting PCCO thin films can be grown. Attempts at growing a-axis and (110) oriented superconducting PCCO films have not been successful. Since we want to tunnel into the *ab*-plane of this material and the thickness of the films is only $3000\mathring{A}$, a great deal of difficulty is encountered, not only in positioning the normal metal tip on the edge of the film, but also in varying the contact pressure without the tip slipping off the film edge. Hence, we have devised an alternative technique for PCS in the *ab*-plane of thin films and have designed and constructed a new probe for this purpose. We also note that a variation of this alternative method has been employed successfully in the past for PCS on superconductors [37].

A schematic side view of our point contact technique is depicted in Fig. 2. The film is cleaved in air to expose a fresh edge, electrical contacts on the film are made with Ag-In and it is glued with a quick-setting epoxy to a sapphire base. The film is placed in our PCS probe and a Au or Pt-Rh alloy wire of $0.25mm$ diameter, oriented perpendicular to the plane of the film, is carefully brought into contact with the cleaved edge of the film. The point contact junction is formed between the wire and the sharp edge of the film. The PCS probe is placed in a Helium-4 bath which can be pumped down to $1.4\ K$. In order to study the effect of the magnetic field on the point contact spectra and to drive the PCCO into the normal state, the film is placed with its ab-plane perpendicular to the magnetic field. In this orientation the H_{c2} of our optimally-doped PCCO films is $8\ T$ (at $1.4\ K$) and this ensures that the film goes into the normal state at fields achievable in our laboratory. Therefore, a bevel gear arrangement is required to change the direction of motion for the

point contact to be made. The Au or Pt-Rh wire is glued to a sapphire piece which in turn is glued to the threaded 'nut' on the shaft. The bevel gears can be rotated from outside of the Helium-4 bath. When the bevel gears rotate, the 'nut' along with the wire moves towards the edge of the film. The point contact can be made this way and the pressure of the contact can also be varied. A high pitch anti-backlash worm gear arrangement at the top part of the probe outside the Helium-4 bath ensures that the distance between the wire and the film edge can be controlled to sub-micron precision. One important advantage of this method over the 'spear on anvil' method is that the point contact is relatively stable against mechanical perturbations because the wire is also supported by the edge of the substrate. We make a four probe measurement to obtain the $(I-V)$ characteristics of our junctions and numerically differentiate it to obtain the conductance. We also use a standard lock-in technique to obtain the $G-V$ spectra directly.

III. RESULTS AND DISCUSSION

Since our method of making point contact is unconventional, we decided to demonstrate its validity and effectiveness by doing PCS on optimally-doped c-axis oriented YBCO thin films in the same configuration that we have used for PCS on PCCO. The reasons for choosing YBCO for this purpose are that YBCO is an HTSC like PCCO and there is a consensus that the pairing symmetry of optimally-doped YBCO is predominantly d-wave and a ZBCP due to ABS has been observed in tunnel junctions and point contact junctions [4,17,38,39]. The YBCO films have a thickness of 2000 $\mathring{A}$ and were grown on STO and Neodymium Gallium Oxide (NGO) substrates. The films have T_c in the range $89.5 \pm 0.5K$. Since the $G-V$ spectra for a superconductor with d-wave pairing symmetry are orientation-dependent, the films were cleaved in different directions. However, we find no major difference in the features of the $G-V$ spectra for different cleavage orientations which suggests that surface roughness at the atomic scale leads to averaging of contributions from facets oriented in various directions.

Figure 3 shows the $G-V$ characteristics for point contact tunneling into the ab-plane of YBCO with Pt-Rh alloy wire as the counter-electrode. One can see from the zero field data that the width of the ZBCP is 6 meV and the coherence peaks appear at the gap value of 18 meV. This is qualitatively similar to what is observed in PCS and Scanning Tunneling Spectroscopy (STS) on YBCO thin films and crystals [38,39] and confirms the validity and effectiveness of our point contact method.

We also studied the effect of c-axis oriented magnetic field on the ZBCP as shown in Fig. 3. We saw no splitting of the ZBCP at low fields unlike what has been reported for tunnel junctions [4,17]. We observe that the peak splits explicitly in a magnetic field of 8 T. The origin of the ZBCP splitting in YBCO is still a matter of debate [4,17]. However, direct splitting of the ZBCP in a magnetic field has not been observed in other tunneling experiments [7,19]. Two of the possible reasons for the absence of splitting of the ZBCP at low fields are that the orientation of the films and surface morphologies of the junction interface are different from those in tunneling experiments in Ref. [4,17]. In our experiment, the magnetic field is along the c-axis and perpendicular to the plane of film. Therefore, vortices enter the film even at very low magnetic fields due to the large demagnetization factor and hence the Meissner currents become almost field independent.

The entry of vortices into the film at low fields probably marginalizes the role that Meissner currents are expected to play in the splitting of the ZBCP. Also, it is theorized that the splitting due to a sub-dominant order parameter (is or id_{xy}) may be suppressed for rough junction interfaces, especially if the sub-dominant order parameter is id_{xy} [40]. A third reason for the absence of splitting at low fields in our experiment may be that the splitting of the ZBCP is expected to occur above a critical field whose magnitude is proportional to the transmissivity of the junction [41]. Furthermore, the transmission coefficient decreases exponentially with increasing barrier strength [42]. Since our point contact junction is more transparent than a tunnel junction, the fields for which we observe splitting are larger than those observed in experiments with tunnel junctions. We also note that the magnitude of the splitting is 2.1 meV at 8 T in our experiment which is in fairly good agreement with the magnitude of the indirect splitting in Ref. [7]. The above discussion on the splitting of the ZBCP in a magnetic field has important implications for our data on PCCO.

We have performed a systematic and exhaustive study of PCS in the *ab*-plane of superconducting PCCO thin films of different cerium concentrations and have observed the $G-V$ spectra for different barrier strengths and in magnetic fields. We have made point contacts on films with different nominal cleavage orientations. More than fifty point contact junctions have been studied.

For PCS in PCCO films with 0.13 cerium concentration, we observe a ZBCP at low junction resistances and we have studied the ZBCP in a magnetic field applied normal to the ab-plane of the film. The data is shown in Fig 4. The shape and magnitude of the ZBCP suggest that it originates due to ABS and we have fitted the zero field data to a calculated d-wave $G-V$ spectrum in Fig 4a. The fit takes into account the temperature dependence of the Fermi function. Besides the gap value (Δ) and the barrier strength (Z), the fitting parameters include the quasiparticle lifetime broadening parameter (Γ), and the angle between the normal to the junction interface and the direction of the maximum gap (α). The ZBCP is completely suppressed for magnetic fields in excess of H_{c2} which is about 4 T, lending further support to the argument that the ZBCP is related to the superconductivity of the PCCO. Compared to the $G-V$ spectra on YBCO, the ZBCP is not accompanied by a gap-like feature because of the low barrier strength of this normal metal/PCCO junction. The magnitude and width of the ZBCP decreases with increasing magnetic field [43] and the ZBCP does not split. The possible reasons for the absence of splitting of the ZBCP in PCCO are the same as those advanced earlier for YBCO. Moreover, the fact that we do not observe splitting of the ZBCP at all in PCCO may be due to a combination of two phenomena: low Z of our junction and the low H_{c2} of PCCO compared to YBCO. Therefore, the absence of splitting of the ZBCP in a magnetic field in under-doped PCCO is not unexpected.

Fig. 5 shows some representative $G-V$ spectra for PCCO $x=0.13$ for different junction resistances. For a high junction resistance which implies a higher barrier strength, we observe a gap-like feature with coherence peaks at the gap value. This can be seen more clearly in the inset (Fig. 5a). As the junction resistance is decreased, a ZBCP appears along with the gap-like feature shown in greater detail in the inset (Fig. 5b). For even lower junction resistance (and lower Z), a pronounced ZBCP is seen whose width is the same as the value of the gap as deduced from the fit in Fig. 4a. We have observed ZBCPs for low junction resistances in approximately 30 percent of our junctions and we believe the ZBCP appears when the normal metal electrode is able to penetrate the native surface barrier and make

direct contact with the superconductor. For a junction with high barrier strength in a d-wave superconductor, theory predicts a sharp and pronounced ZBCP (see Fig. 1b) which we have never observed in our experiments on high Z junctions.

How do we explain this unusual Z-dependence of the $G-V$ spectra? One possibility is the presence of an induced order parameter at the surface for junctions with low transmission coefficient (i.e. high Z). This suggestion is based on the paper by Tanuma *et al.* [44] who have proposed that for a high-Z junction in a d-wave superconductor, the $d_{x^2-y^2}$ order parameter is suppressed at the surface and the spectral weight is transferred to a sub-dominant is or id_{xy} order parameter. This effect is maximum for tunneling into (110) orientation of the junction interface. We believe that in the case of PCCO, the magnitude of this induced order parameter exceeds the bulk $d_{x^2-y^2}$ order parameter at the surface, which is plausible according to the theoretical calculations in Ref. [44]. Therefore, we attribute the gap-like feature in the high-Z limit to an induced order parameter whose magnitude ranges between 3 meV and 5 meV as estimated from the separation of the coherence peaks in several of the $G-V$ spectra (for example, see Fig. 5a). We note that this induced order parameter is not present in the low-Z junctions and the ZBCP we observe is due to the d-wave nature of the bulk order parameter whose magnitude from the fit in Fig. 3a is 6 meV. Another possible explanation for the absence of the ZBCP in junctions with high-Z is that disorder suppresses the ZBCP. This is based on the results of the experiment on tunnel junctions on YBCO in which the effect of disorder on the ZBCP was studied [45]. However, in that experiment, the gap-like feature disappears along with the ZBCP as disorder increases. Since a pronounced gap-like feature is seen in our high-Z data, we think it is unlikely that the absence of a ZBCP is solely due to disorder.

Although the simplest and most likely explanation of the ZBCPs in under-doped PCCO junctions is the d-wave pairing symmetry, we want to point out that ZBCPs due to ABS are predicted for other exotic symmetries (e.g. extended s-wave, $d+s$ with $d>s$) [13]. The surface orientation dependence of the $G-V$ spectra predicted for the above order parameters is different for each one but we are unable to distinguish between these by our experimental method because our $G-V$ spectra are an average of contributions from facets of various orientations on the atomic scale. The existence of roughness at the atomic scale is supported by our observation that we find no qualitative change in the spectra for tunneling into different surface orientations.

The point contact spectra for optimally-doped and over-doped PCCO for different junction resistances are shown in Fig. 6 and Fig. 7 respectively. The $G-V$ features are similar for these two doping levels and we will discuss these together. For high resistance junctions we see gap-like features with coherence peaks at the gap values. This is consistent with previous PCS and tunneling experiments on optimally-doped NCCO and PCCO [5–7] where no ZBCP was observed. For lower junction resistances and hence lower barrier strengths, we do not observe a ZBCP which suggests the absence of ABS at the Fermi energy. The shape of $G-V$ spectra are now influenced by Andreev reflections and qualitatively resemble those of s-wave superconductors in the low/intermediate Z limit (see Fig. 1a). In general, a dip in the conductance at zero bias in low Z junctions suggests absence of nodes in the order parameter [49]. Therefore, keeping in view the shape of our $G-V$ spectra for low Z junctions on under-doped, optimally-doped and over-doped PCCO, we propose a transition from a d-wave order parameter for under-doped PCCO to a nodeless gap for optimal and

over-doped PCCO. As an example, we have fitted the $G-V$ data for the lowest junction resistance on over-doped PCCO to the generalized BTK model with isotropic gap as shown in Fig. 8a. A slightly better fit is obtained with a $d+is$ pairing symmetry calculation, with equal weights of the real and imaginary parts of the order parameter as shown in Fig. 8b. Both fits include the effect of thermal broadening. In calculating the best fit to the data, the lifetime broadening parameter (Γ) is kept as small as possible and the angular integral is taken over the full range $-\pi/2 < \theta < \pi/2$. The purpose of the fits is to show that in both models the s-wave component has the same magnitude and that the low bias characteristics of the $G-V$ spectra are determined to a large extent by the s-wave component of the order parameter. We also tried a fit to $d+id_{xy}$ pairing symmetry model with the same constraints on Γ and θ as in the $d+is$ model. However, given the physically reasonable constraints on Γ and θ, the data could not be fit to the $d+id_{xy}$ model.

Our data points to a transition in pairing symmetry with doping and this suggests the existence of a Quantum Critical Point (QCP) at or near optimum doping. For d-wave superconductors, theoretical considerations limit the pairing symmetry transition across a QCP from d-wave to either $d+is$ or $d+id_{xy}$ [50]. Our low Z data on PCCO is more consistent with a d to $d+is$ pairing symmetry transition across a QCP near optimum doping. A recent report also suggests a transition in pairing symmetry across a QCP near optimum doping in YBCO. [4].

It has been suggested that the proximity effect for transparent junctions on $d_{x^2-y^2}$ superconductors leads to an induced s-wave order parameter in the normal electrode [47,48]. This effect is maximum for (100) or (010) surface orientations and does not occur for (110) orientation. If the absence of a ZBCP in our low Z data on optimally-doped and over-doped PCCO is attributed to an s-wave order parameter being induced in the normal electrode due to the proximity effect, then it is difficult to understand why this effect is not observed in our low Z junctions on under-doped PCCO. Therefore, we do not think our data can be explained by an s-wave order parameter induced by the proximity effect. Hence, the $d+is$ order parameter appears to be a property of the surface of optimally-doped and over-doped PCCO.

One interesting and puzzling aspect is the dependence of the gap-like features on the barrier strength and this can be seen in Fig. 6 as well as in Fig. 7. The energy scale of the gap-like features is equal to half the separation of the coherence peaks or maxima on either side of zero voltage bias. For over-doped PCCO, the energy of the gap-like feature in the tunneling limit is 3.2 meV while in the low Z limit we obtain a value of 1.4 meV. For optimally-doped PCCO, the energy of the gap-like feature in the tunneling limit is 5 meV while in the low Z limit it is 3.3 meV. We do not fully understand this phenomenon. However, we attempt to give a reasonable explanation. It is possible that the effect of nano-scale roughness at the place of the junction and the extent of the tunneling cone for quasiparticle injection change with the barrier strength. This may lead to gap-like features appearing at somewhat different energies in the spectra for junctions with different barrier strengths.

We have also studied the dependence of the $G-V$ spectra in the tunneling limit on the magnetic field applied perpendicular to the plane of the film (i.e. parallel to the c-axis of the film) and present our data in Fig. 9a and 9b. Note that the coherence peaks are completely suppressed at 3 T for optimally-doped PCCO and 2 T for over-doped PCCO.

These fields are less than H_{c2} which is 8 T for optimally-doped PCCO and 4 T for over-doped PCCO. We have no explanation for this unusual field dependence at the present time. Notice that the magnitude of the superconducting gap decreases with increasing magnetic field and it evolves into a gap-like feature, qualitatively different from the superconducting gap, at $H \simeq H_{c2}$. We interpret this dip in the density of states at the Fermi energy as a normal state gap whose origin has not yet been determined conclusively and which has been discussed in detail in one of our earlier papers [46].

Finally, we would like to comment on whether our point contact junctions are in the ballistic (or Sharvin) limit i.e the contact radius (a) is much less than the mean free path (l) [51]. This is considered an important criteria for the validity of PCS. The Sharvin formalism was originally developed to model transport across a micro-constriction between two similar metals [52]. This formalism was extended by Wexler to the case where the micro-constriction has a ballistic as well as a thermal (Maxwell) part [53]. Both the Sharvin and Wexler formulas have been employed in previous works for calculating the contact radii for point contact junctions between a metal and an HTSC. However, there is much debate on whether the Sharvin and Wexler formulas are applicable in their present forms to a point contact junction between two materials with very different Fermi liquid parameters and resistivities [54,55], as is the case with a normal metal and a high T_c superconductor. Moreover, since the high T_c superconductors have low mean free paths of the order of tens to hundreds of angstroms, the criterion for point contacts being in the Sharvin limit ($a << l$), as estimated from the Sharvin and Wexler formalisms, have rarely been strictly achieved and in most cases the contact radius is either comparable to or greater than the mean free path in the superconductor [22,38,56,57]. Authors have explained this by either considering the less rigorous condition ($a < l$) as sufficient for a ballistic contact, or suggesting that this leads to a higher effective Z, or postulating the existence of several parallel ballistic contacts. Whatever the case may be, there is some agreement that if the point contact is dominated by the thermal part, its conductance will decrease appreciably at higher voltage bias ($eV > \Delta$) due to localized heating [12,51,56,58]. In our $G - V$ spectra, the conductance at higher voltage bias is either flat or increasing with voltage. Thus, we conclude that our point contact junctions are not in the Maxwell regime and the quasi-particle transport through the junctions is predominantly ballistic. This is a sufficient condition for energy-resolved spectroscopy of point contact junctions.

IV. CONCLUSION

For *low barrier strength junctions* on under-doped PCCO, we observe a ZBCP and show that it is due to d-wave pairing symmetry. We do not observe a ZBCP in low Z PCS data on optimally-doped and over-doped PCCO and this indicates absence of nodes in the gap. Our data, along with theoretical considerations, indicates a $d + is$ pairing symmetry for optimally-doped and over-doped PCCO. We find that our data for low barrier strength junctions for all doping levels can be best explained by a d- to $d + is$ pairing symmetry transition across optimum doping. This indicates the presence of a QCP near optimum doping for PCCO.

We observe gap-like features for *high barrier strength junctions* for all doping levels. For high Z junctions on under-doped PCCO, we believe that the d-wave order parameter is

suppressed at the surface and the spectral weight is transferred to an is order parameter which leads to gapped spectra. For high Z junctions on optimally-doped and over-doped PCCO, the gap-like features are due to a fully gapped Fermi surface. The data on low Z junctions on over-doped PCCO suggests that a $d+is$ order parameter leads to this nodeless and fully gapped Fermi surface. Indeed, data from all the previous PCS and tunneling experiments on NCCO and PCCO, which consistently showed a gap-like feature can be explained by an induced is order parameter at the surface of under-doped PCCO, and by an order parameter without nodes for optimally-doped and over-doped PCCO.

We have studied the $G-V$ spectra in magnetic fields up to and greater than H_{c2} of PCCO. We find that the ZBCP in the $G-V$ spectra of under-doped PCCO does not split in magnetic fields up to H_{c2}. This may be due to one or more of the following reasons: immediate penetration of vortices into our films; surface roughness of our junctions; the high transmissivity of our junctions. For $H > H_{c2}$, we observe a normal state gap at the Fermi energy in the $G-V$ spectra in the tunneling limit for optimally-doped and over-doped PCCO. The normal state gap is of the same order of magnitude as the superconducting gap but differs qualitatively from it. The normal state gap is at least an order of magnitude less than the pseudo-gap that has been observed in other experiments on NCCO [59,60].

The authors acknowledge useful discussions with C. J. Lobb, S. M. Anlage and P. Fournier. We would like to thank the following colleagues: J. S. Higgins and M. C. Sullivan for assistance with PCCO and YBCO film growth, and Hamza Balci and Z. Y. Li for some of the PCCO ceramic pellets. This work was supported in part by NSF DMR 01-02350.

REFERENCES

[1] Guy Deutscher and Roger Maynard in: The gap symmetry and fluctuations in high T_c superconductors, ed. Julien Bok *et al.*, (Plenum Press, New York, 1998)
[2] Satoshi Kashiwaya and Yukio Tanaka, Rep. Prog. Phys. **63**, 1641 (2000)
[3] C. C. Tsuei and J. R. Kirtley, Rev. Mod. Phys. **72**, 969 (2000)
[4] Y. Dagan and G. Deutscher, Phys. Rev. Lett. **87**, 177004 (2001)
[5] Q. Huang *et al.*, Nature **347**, 369 (1990)
[6] S. Kashiwaya *et al.*, Phys. Rev. B **57**, 8680 (1998)
[7] L. Alff *et al.*, Eur. Phys. J. B **5**, 423 (1998)
[8] C. C. Tsuei and J. R. Kirtley, Phys. Rev. Lett. **85**, 182 (2000)
[9] J. D. Kokales *et al.*, Phys. Rev. Lett. **85**, 3696 (2000)
[10] R. Prozorov *et al.*, Phys. Rev. Lett. **85**, 3700 (2000)
[11] G. E. Blonder, M. Tinkham and T. M. Klapwijk, Phys. Rev. B **25**, 4515 (1982)
[12] G. E. Blonder and M. Tinkham, Phys. Rev. B **27**, 112 (1983)
[13] Yukio Tanaka and Satoshi Kashiwaya, Phys. Rev. Lett. **74**, 3451 (1995)
[14] Chia-Ren Hu, Phys. Rev. Lett. **72**, 1526 (1994)
[15] M. Fogelström *et al.*, Phys. Rev. Lett. **79**, 281 (1997)
[16] R. Krupke and G. Deutscher, Phys. Rev. Lett. **83**, 4634 (1999)
[17] M. Covington *et al.*, Phys. Rev. Lett. **79**, 277 (1997)
[18] Satoshi Kashiwaya *et al.*, Phys. Rev. B **53**, 2667 (1996)
[19] J. W. Ekin *et al.*, Phys. Rev. B **56**, 13746 (1997)
[20] F. Hayashi *et al.*, J. Phys. Soc. Jpn **67**, 3234(1998)
[21] A. Mourachkine, Europhys. Lett. **50**, 663(2000)
[22] Amlan Biswas *et al.*, Phys. Rev. Lett. **88**, 207004 (2002)
[23] D. H. Wu *et al.*, Phys. Rev. Lett. **70**, 85(1993)
[24] A. Andreone *et al.*, Phys. Rev. B **49**, 6392 (1994).
[25] C. W. Schneider *et al.*, Physica C **233**, 77 (1994)
[26] L .Alff *et al.*, Phys. Rev. Lett. **83**, 2644(1999)
[27] John A. Skinta *et al.*, Phys. Rev. Lett. **88**, 207005 (2002)
[28] N. P. Armitage *et al.*, Phys. Rev. Lett. **86**, 1126(2001)
[29] T. Sato *et al.*, Science **291**, 1517 (2001)
[30] G. Blumberg *et al.*, Phys. Rev. Lett. **88**, 107002 (2002)
[31] R. W. Hill *et al.*, Nature **414**, 711 (2001)
[32] Hamza Balci *et al.*, Phys. Rev. B **66**, 174510 (2002)
[33] E. Maiser *et al.*, Physica C **297**, 15 (1998)
[34] J. L. Peng *et al.*, Phys. Rev. B **55**, R6145 (1997)
[35] H. Van Kempen in: Scanning Tunneling Microscopy and Related Methods, ed. R. J. Behm *et al.* (Kluwer Academic Publishers 1990)
[36] I. K. Yanson, Sov. J. Low Temp. Phys. **17**, 143 (1991)
[37] R. C. Reinertson *et al.*, Physica C **200**, 377 (1992)
[38] J. Y. T. Wei *et al.*, Phys. Rev. Lett. **81**, 2542 (1998)
[39] A. Sharoni *et al.*, Phys. Rev. B **65**, 134526 (2002)
[40] D. Rainer *et al.*, J. Phys. Chem. Solids **59**, 2040 (1998)
[41] Yukio Tanaka *et al.* J. Phys. Soc. Jpn, **71**, 2005 (2002)

[42] E. L. Wolf, Principles of electron tunneling spectroscopy (Oxford University Press, New York, 1985)
[43] The decrease in width and height of the ZBCP with magnetic field is probably due to the decrease in magnitude of the superconducting gap. This is under further investigation.
[44] Y. Tanuma *et al.*, Phys. Rev. B **64**, 214519 (2001)
[45] M. Aprili *et al.*, Phys. Rev. B **57**, R8139 (1998)
[46] Amlan Biswas *et al.* Phys. Rev. B **64**, 104519 (2001)
[47] Yoji Ohashi, J. Phys. Soc. Jpn. **65**, 823 (1996)
[48] Amir Kohen and Guy Deutscher, cond-mat/0207382 (2002)
[49] Guy Deutscher *et al.*, Physica C **282-287**, 140 (1997)
[50] Matthias Vojta *et al.*, Phys. Rev. Lett. **85**, 4940 (2000)
[51] A. M. Duif *et al*, J. Phys. Condens. Matter **1**, 3157 (1989)
[52] Yu. V. Sharvin, Zh. Eksp. Teor. Fiz. **48**, 984 (1965) [Sov. Phys. JETP **21**, 655 (1965)]
[53] G. Wexler, Proc. Phys. Soc. London **89**, 927 (1966)
[54] K. Gloos, Phys. Rev. Lett. **85**, 5257 (2000)
[55] Ch. Wälti *et al.*, Phys. Rev. Lett. **85**, 5258 (2000)
[56] R. S. Gonnelli *et al.*, Eur. Phys. J. B **22**, 411 (2001)
[57] A. I. D'yachenko *et al.*, Phys. Rev. B **61**, 1500 (2000)
[58] K. Hasselbach *et al.*, Phys. Rev. B **46**, 5826 (1992)
[59] N. P. Armitage *et al.*, Phys. Rev. Lett. **87**, 147003 (2001)
[60] Y. Onose *et al.*, Phys. Rev. Lett. **87**, 217001 (2001)

FIGURES

FIG. 1. (a) Calculated $G-V$ curves for an s-wave superconductor at zero Kelvin using the BTK model (Ref. [11]). (b) Calculated $G-V$ curves for a d-wave superconductor at zero Kelvin for tunneling into (110) orientation (Ref. [13]).

FIG. 2. A schematic side view of our point contact method.

FIG. 3. $G-V$ characteristics for optimally-doped YBCO taken at T=4.23 K in a magnetic field applied parallel to the c-axis. The spectra are shifted for clarity.

FIG. 4. $G-V$ characteristics for under-doped PCCO at T = 1.43 K showing the variation of the ZBCP with magnetic field applied parallel to the c-axis. The spectra are shifted for clarity. Inset(a): a fit of the ZBCP data (circles) to the calculated conductance for a normal metal/$d_{x^2-y^2}$ superconductor (solid line). The fitting parameters are discussed in the text.

FIG. 5. $G-V$ spectra for different junction resistances for under-doped PCCO at T = 1.43 K. The conductance is normalized to the normal state conductance and the spectra are shifted for clarity. Inset (a) shows in detail the high Z data with $R_N = 46.4\Omega$. Inset (b) shows in detail the spectrum with normal state resistance of 28.7 Ω. Note that both the superconducting gap and ZBCP are clearly visible and compare with the zero field data for YBCO in Fig. 3.

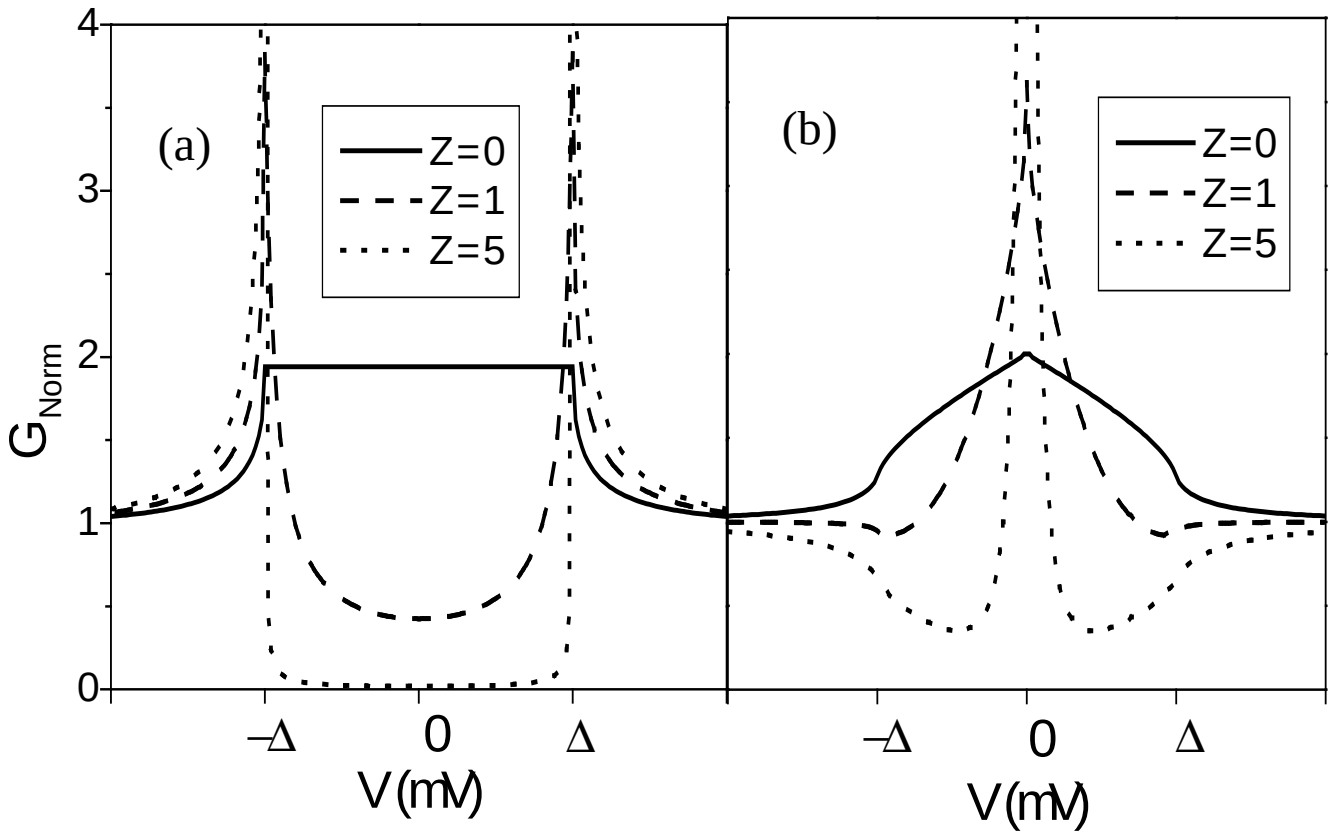
FIG. 6. $G-V$ spectra for different junction resistances for optimally-doped PCCO at T = 1.43 K. The conductance is normalized to the normal state conductance and the spectra are shifted for clarity.

FIG. 7. $G-V$ spectra for different junction resistances for over-doped PCCO at T = 1.43 K. The conductance is normalized to the normal state conductance and the spectra are shifted for clarity.

FIG. 8. (a) A fit of the low resistance $G-V$ spectrum (circles) for over-doped PCCO to the generalized BTK model with an isotropic gap (solid line).(b) A fit of the same data to $d+is$ pairing symmetry model. The fitting parameters are discussed in the text.

FIG. 9. Variation of the $G-V$ characteristics for high resistance junctions with magnetic field applied parallel to the c-axis for (a) optimally-doped PCCO and (b) for over-doped PCCO at T = 1.43 K. The spectra are shifted for clarity.

Fig. 1



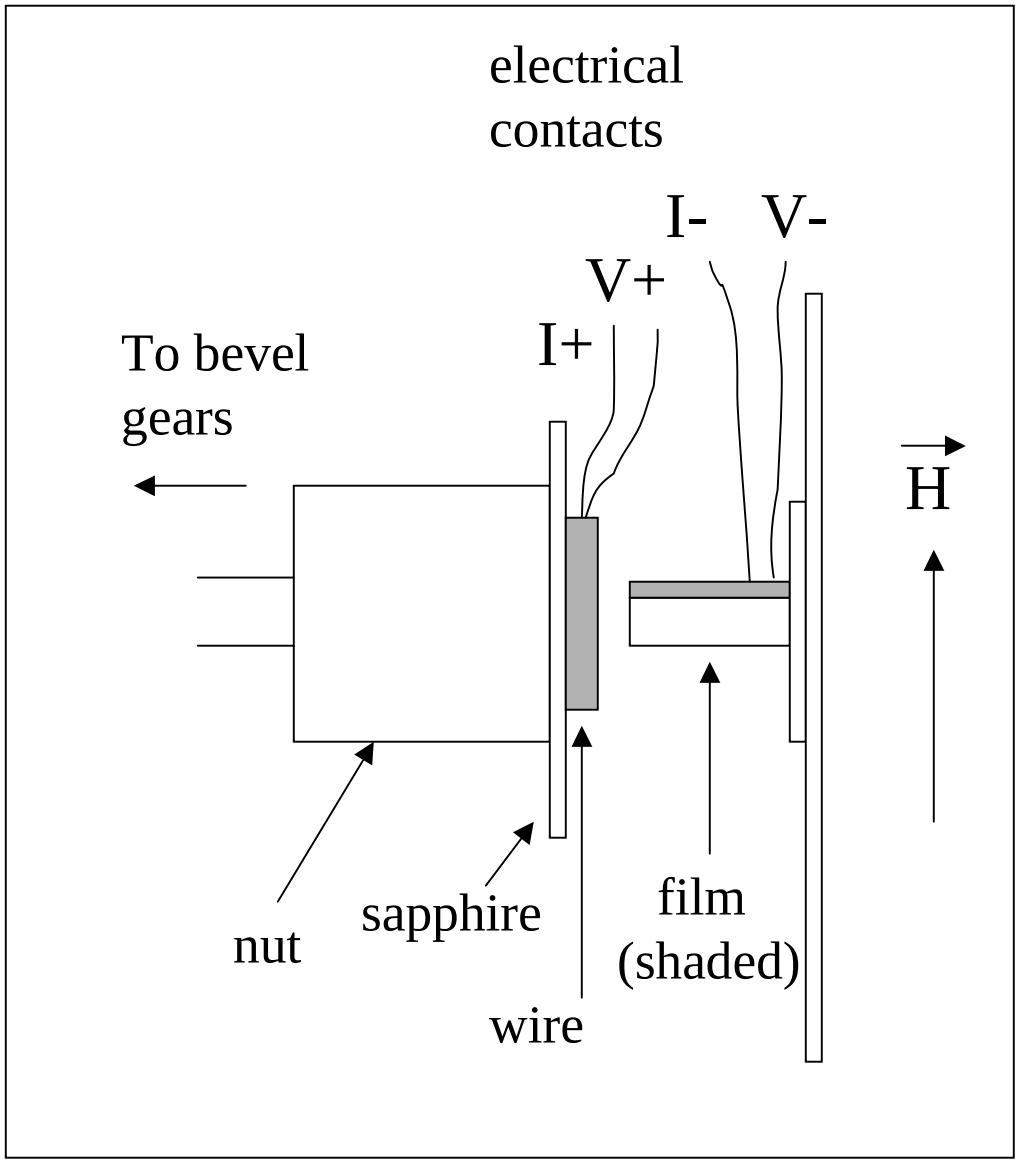

electrical
contacts
I-
V-
V+
I+
To bevel
gears
H
nut
sapphire
wire
film
(shaded)

Fig 2

Fig. 3

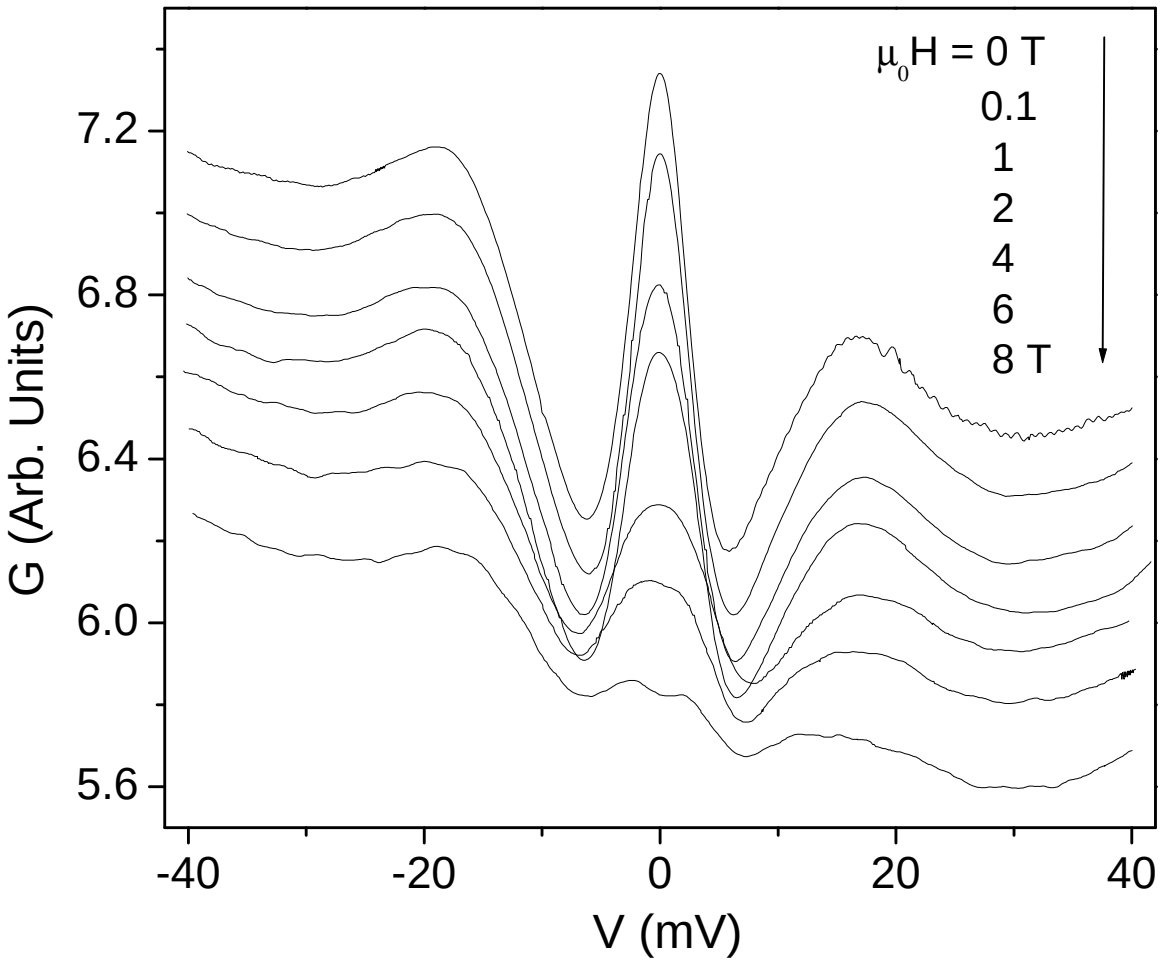


Fig. 4

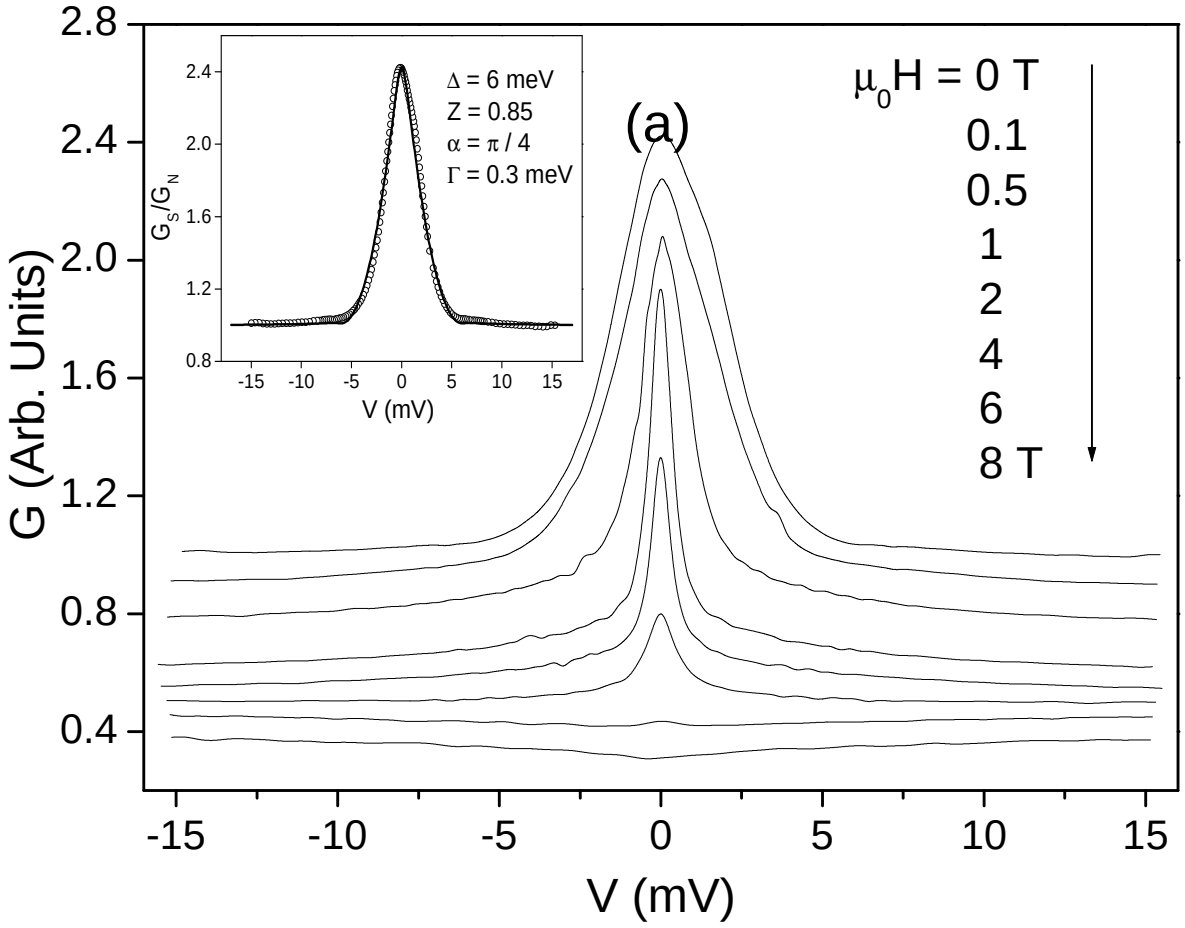

(a)
$\mu_0 H$ = 0 T
0.1
0.5
1
2
4
6
8 T
G (Arb. Units)
V (mV)
G_S/G_N
Δ = 6 meV
Z = 0.85
α = π / 4
Γ = 0.3 meV
V (mV)

Fig. 5

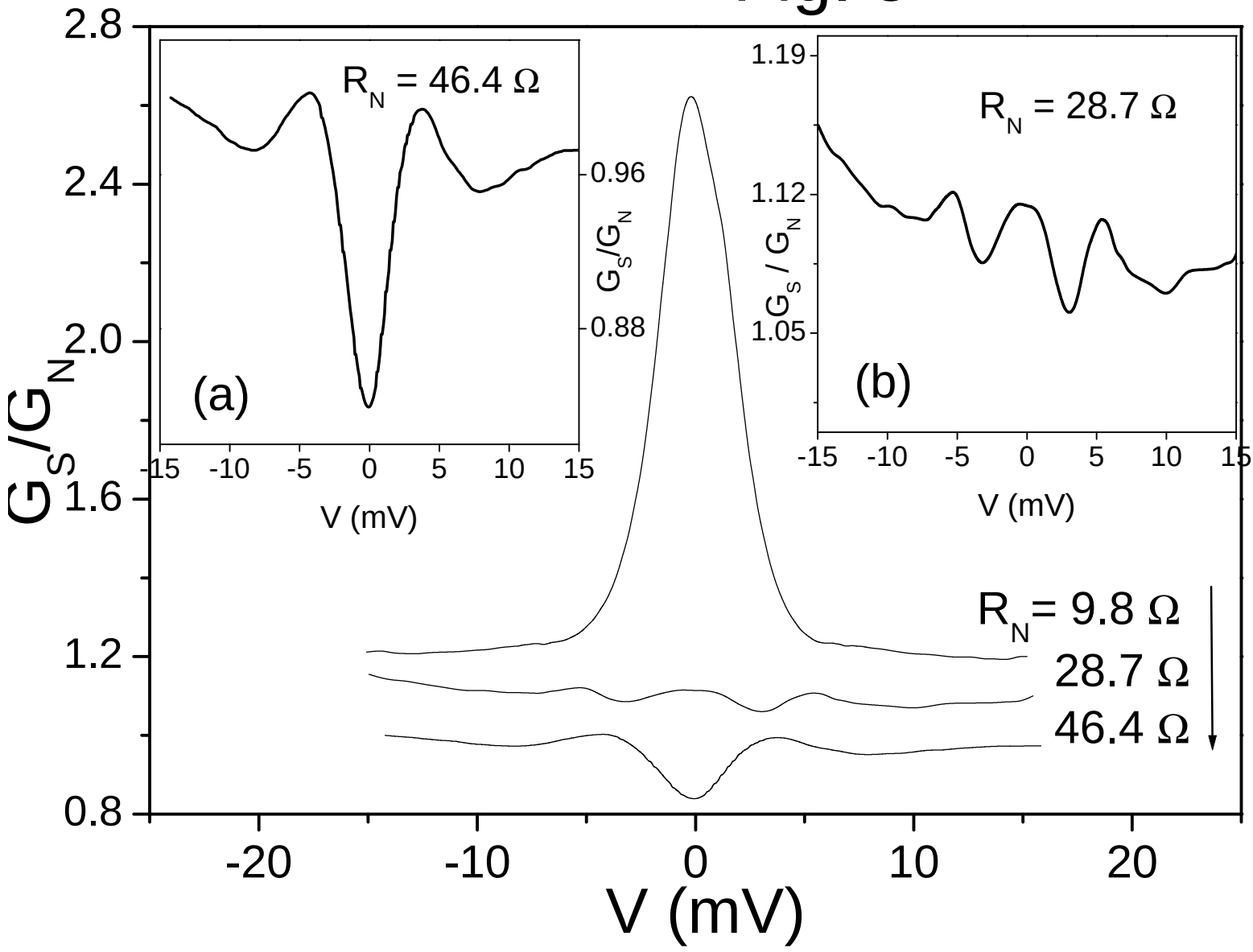

2.8
2.4
2.0
1.6
1.2
0.8
G_S/G_N
-20
-10
0
10
20
V (mV)
R_N = 9.8 Ω
28.7 Ω
46.4 Ω
R_N = 46.4 Ω
(a)
0.96
0.88
G_S/G_N
-15
-10
-5
0
5
10
15
V (mV)
R_N = 28.7 Ω
(b)
1.19
1.12
1.05
G_S / G_N
-15
-10
-5
0
5
10
15
V (mV)

Fig. 6

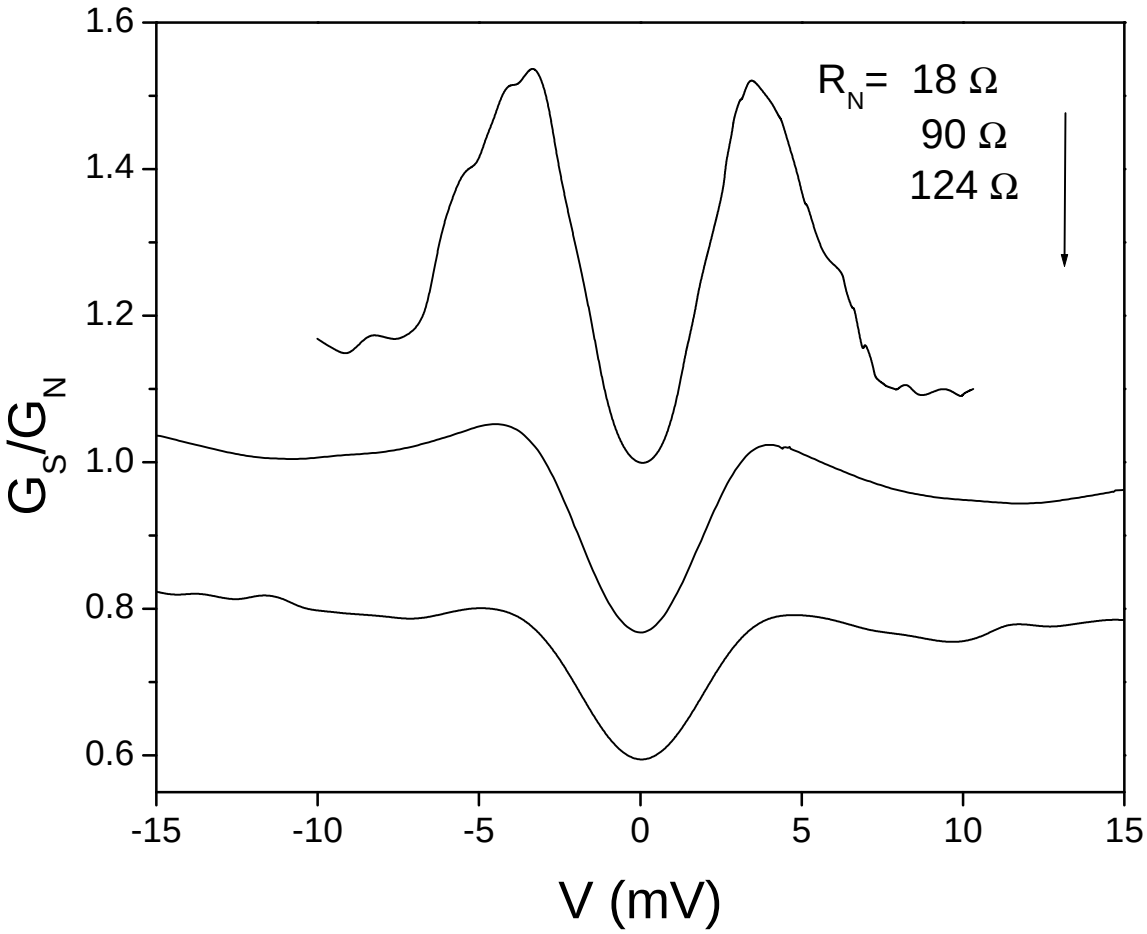


Fig. 7

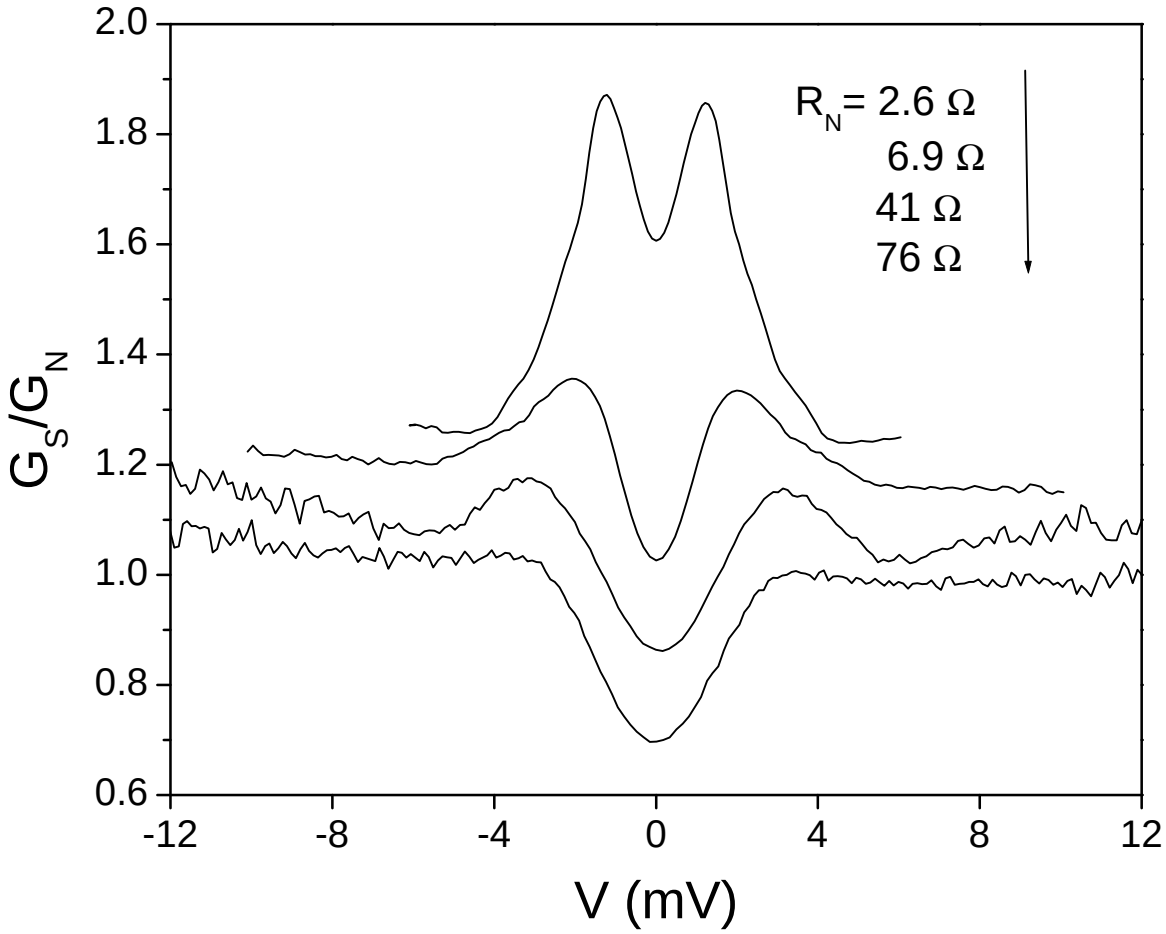
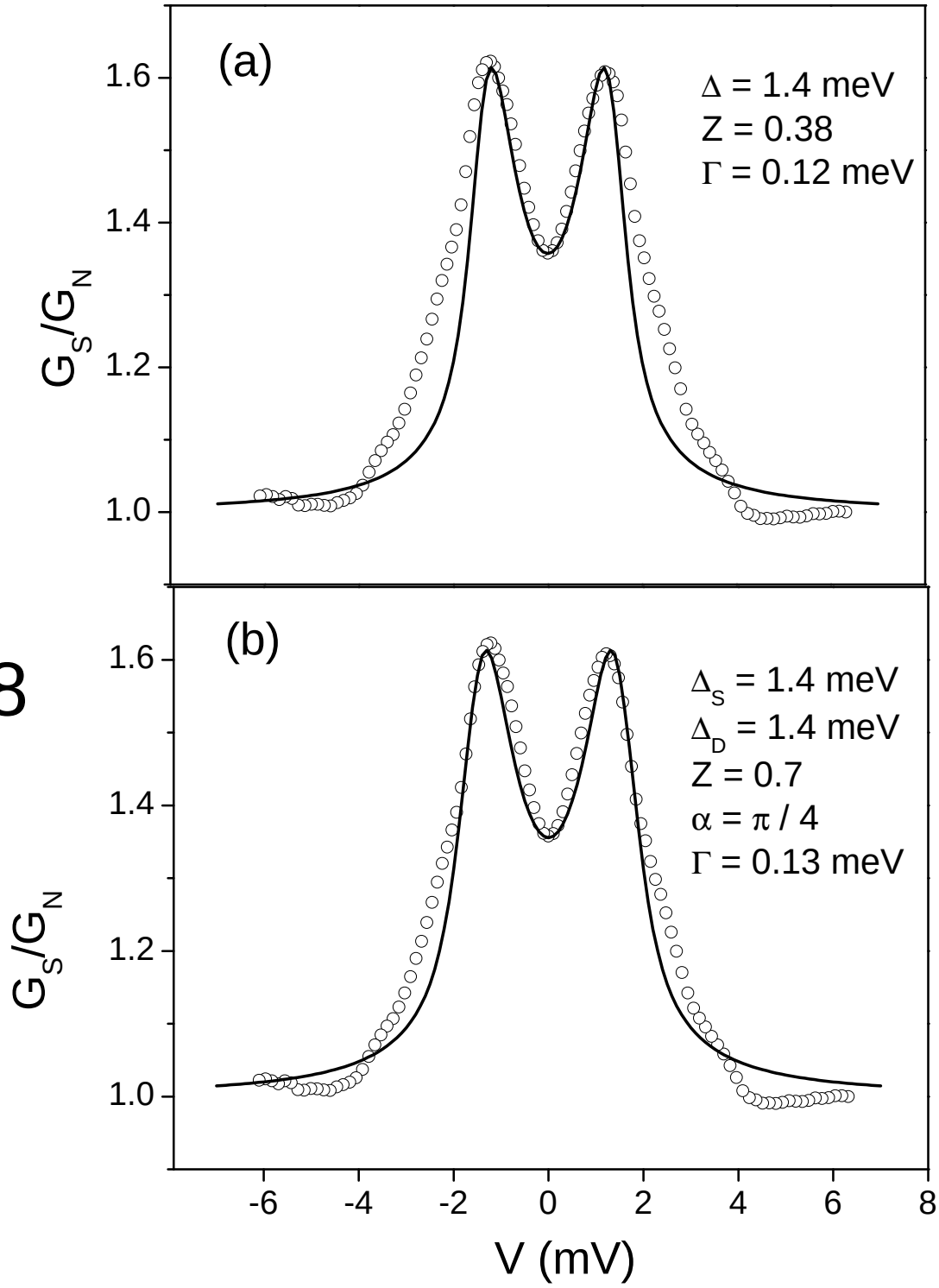


Fig. 8


(a)
Δ = 1.4 meV
Z = 0.38
Γ = 0.12 meV
(b)
Δ_S = 1.4 meV
Δ_D = 1.4 meV
Z = 0.7
α = π / 4
Γ = 0.13 meV
G_S/G_N
1.0
1.2
1.4
1.6
-6
-4
-2
0
2
4
6
8
V (mV)

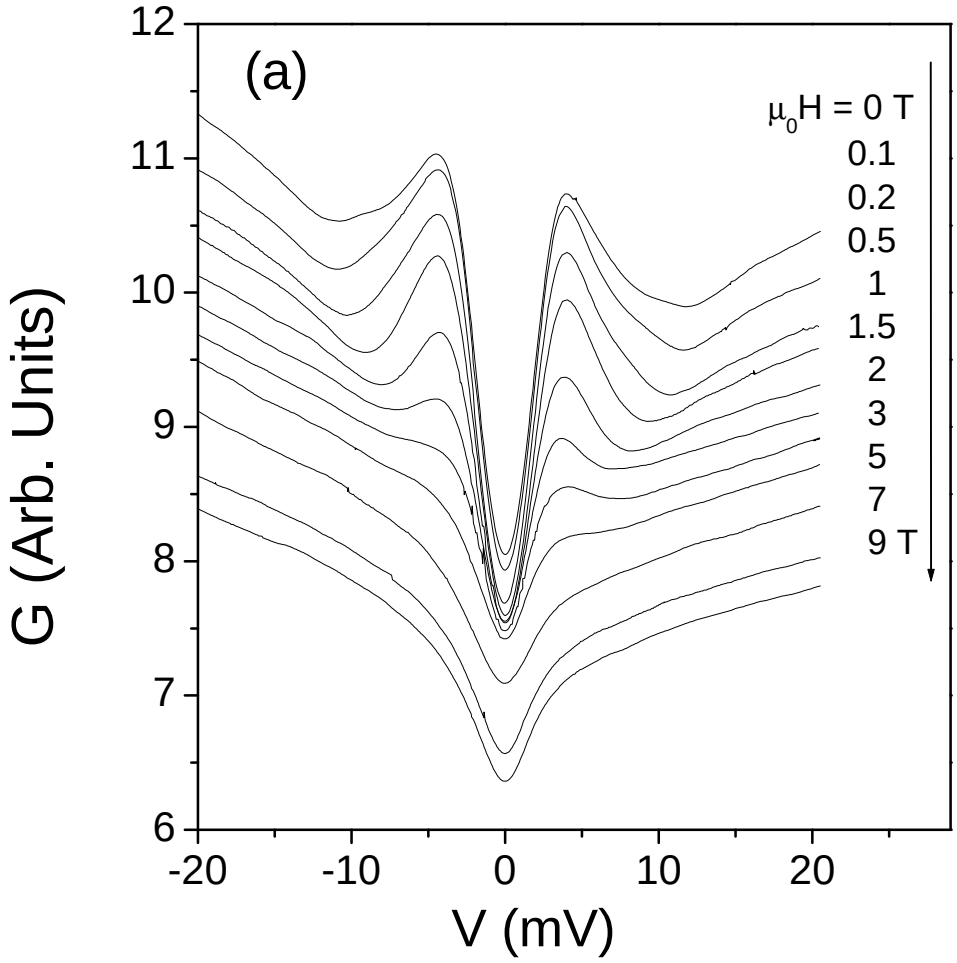
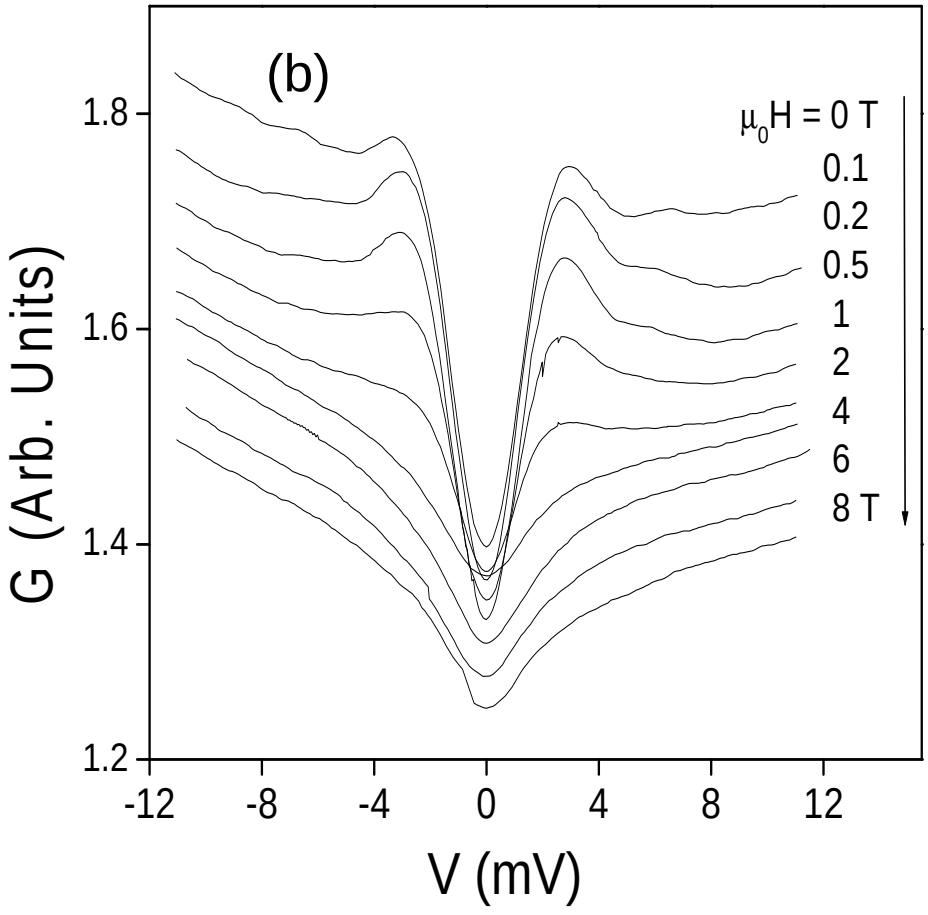

(a)
μ_0H = 0 T
0.1
0.2
0.5
1
1.5
2
3
5
7
9 T
G (Arb. Units)
V (mV)
12
11
10
9
8
7
6
-20
-10
0
10
20

Fig. 9


(b)
μ_0H = 0 T
0.1
0.2
0.5
1
2
4
6
8 T
G (Arb. Units)
V (mV)
1.8
1.6
1.4
1.2
-12
-8
-4
0
4
8
12